

Article

Experimental Value of the Specific Surface Energy of the Cleavage {10.4} Calcite Rhombohedron in the Presence of Its Saturated Aqueous Solution

Emanuele Costa *  and Dino Aquilano

Department of Earth Sciences, Università di Torino, Via Valperga Caluso 35, 10125 Torino, Italy; dino.aquilano@unito.it

* Correspondence: emanuele.costa@unito.it; Tel.: +39-347-2281511

Received: 26 April 2018; Accepted: 28 May 2018; Published: 30 May 2018



Abstract: In this study, we describe a method to obtain experimental values of the surface energy of calcite. A zenithal imaging device was used to acquire pictures of droplets of CaCO_3 saturated aqueous solution on the surface of a calcite crystal sample. Pictures were used to measure the contact angle between the droplets and the {10.4} calcite surfaces. The method is discussed along with its geometrical ground, as well as the theoretical foundation of the contact angle calculation. A comparison is made with the literature data; a good agreement is found between our experimental values and those obtained from the more recent ab initio calculations.

Keywords: calcite; contact angle; surface energy

1. Introduction

Measuring the surface energy of calcite is often obtained using methods involving the determination of the contact angle of various liquids in the system: crystal/liquid/air, but also in submerged systems using non-aqueous solvents. Evaluating the contact angle usually requires sophisticated mechanical and optical devices, to ensure perfect co-planarity of the calcite surface and the optical axis of the camera, the absence of parallax error during the image acquisition, and somewhat ability of the operator regarding the determination of the real angle formed between the calcite face and the droplet boundary at the contact interface [1–3]. The use of a simple experimental device for the collection of zenithal pictures of liquid droplets on mineral surfaces could allow to precisely evaluate both the diameter of a drop of known volume and its contact angle. The acquisition of pictures from a vertical perspective eliminates some problems encountered in traditional imaging of droplet profile, and the rapidity of the operation allows the capture of a great number of images, within a simple experiment run, thus improving the statistics of the measurements. Accordingly, it is worth remembering the reliability of a statistical method when dealing with a real crystal surface. Let us consider the {10.4} crystal surfaces of both a cleaved and an as-grown crystal. At a microscopic level, two different situations are found: the cleaved surface is populated by features of micrometric thickness which interrupt the flatness of the ideal (10.4) terraces, like macrosteps, while in the as-grown surfaces, the thickness of the growth steps decreases down to a nanometric level. As an example, we can observe SEM images of calcite cleavage surface or as-grown calcite surface (Figure 1).

This does not represent a negligible detail, since the contribution of surface steps to the interfacial energy appreciably depends on its height. Consequently, measurements made on a population of droplets settled on different sites of a given crystal surface better represent the interfacial energy value with respect to the one obtained from a single macroscopic drop. Finally, it should not be neglected

that the corresponding calculated values of the interfacial energy are obtained by considering an ideal flat interface (i.e., the only {10.4} terraces, in our case).

When a liquid droplet (in a system solid/liquid/vapor) settles on a solid surface: (i) if the droplet is in mechanical and thermodynamic equilibrium with the substrate and the surrounding vapor phase; and (ii) if the specific adhesion energy between the solid surface and the droplet (β_{adh}) is higher than the specific energy (γ_{lv}) of the liquid–vapor interface, then the contact angle (θ) between the droplet and the surface is higher than 90° . This ensues from the coupling of the Young’s (1) and Dupré’s (1) laws [4–6] where we will define γ_{sv} as the specific energy of the solid–vapor interface, and γ_{sl} as the specific energy of the solid–liquid interface. The latter has been obtained through two independent ways:

$$\gamma_{lv} \cos\theta + \gamma_{sv} = \gamma_{sl} \quad (1)$$

$$\gamma_{lv} + \gamma_{sv} - \beta_{adh} = \gamma_{sl} \quad (2)$$

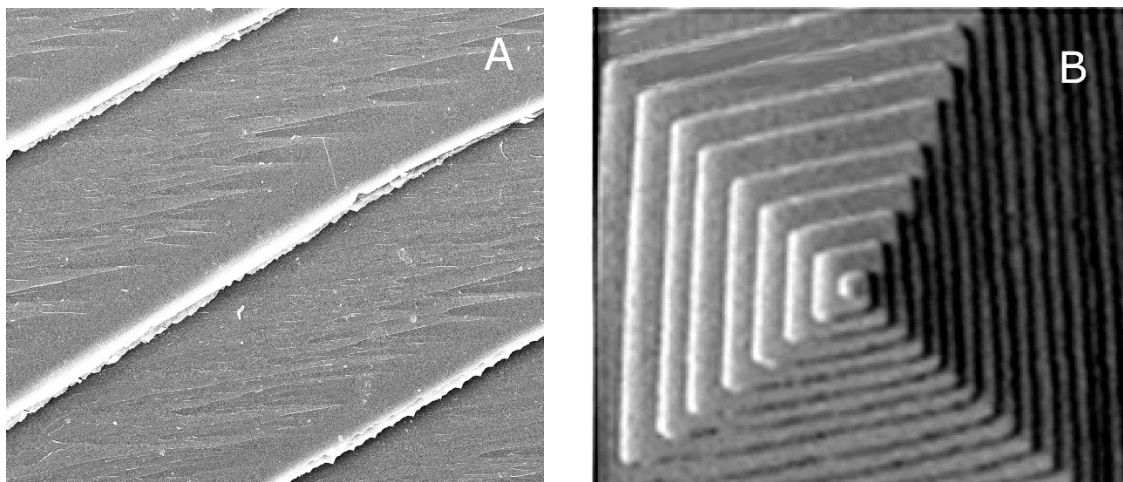


Figure 1. SEM images of calcite crystal surfaces showing features at different scales. (A) A sequence of thin and thick cleavage steps on a {10.4} face of a calcite crystal: the mean step spacing is close to $50 \mu\text{m}$, while the mean height of thick steps is close to $1 \mu\text{m}$. F.O.V. $100 \mu\text{m}$ (by courtesy of Dr. Linda Pastero, private communication); (B) A growth spiral on the {10.4} crystal surfaces of calcite showing monolayered steps (height = 0.3 nm) with mean steps spacing of 30 nm . F.O.V. 600 nm [6].

From Equations (1) and (2) and considering the constraint: $-1 \leq \cos\theta \leq 1$, it follows that the adhesion energy ranges between two limiting values: $0 \leq \beta_{adh} \leq 2\gamma_{lv}$. The minimum ($\beta_{adh} = 0$) corresponds to the situation in which the droplet does not wet the substrate (a water droplet on a hydrophobic surface, for instance). The maximum corresponds to the perfect wetting (the droplet spreads onto the substrate reaching the maximum of its contact area and, consequently, its minimum thickness). In any case, the β_{adh} value cannot exceed the value of the cohesion energy (K_l) of the liquid itself having recollected that $K_l = 2\gamma_{lv}$. It is worth to outline that the θ angle defined in (1) is the angle comprised between the vector representing the interfacial tension γ_{sv} (between the substrate and the vapor) and the vector representing the interfacial tension γ_{lv} (between the liquid droplet and the vapor); this is to avoid any confusion about the sign of the function $\cos\theta$. In other words, the higher the angle θ , the higher the wetting and, hence, the adhesion energy between the droplet and the substrate (Figure 2).

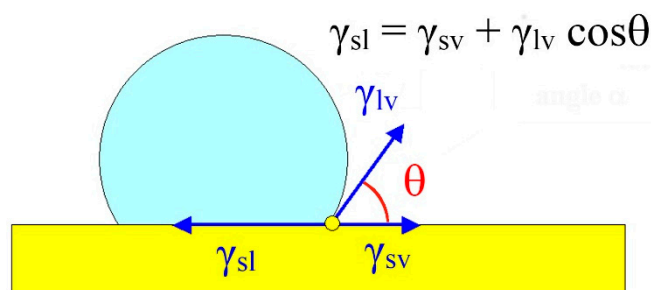


Figure 2. The relationship between the three interfacial tension acting on the boundaries between drop, surface and air (Young's formula).

2. Materials and Methods

2.1. Picture Acquisition

To calculate the contact angle θ , strictly related to β_{adh} , we put a single drop of liquid on a flat surface of the chosen material. The volume of the droplet is a priori constrained, using gas-chromatography syringe, that allows to put down droplets varying from 10 to 100 microliters in volume, with a precision of about half a microliter. The choice of so small volumes is due to the difficulty of obtaining flat and smooth surfaces of natural crystals, large enough to host macro-drops settling on them.

For practical use, a droplet of 20 μL of aqueous solution saturated at room temperature (about 295 K) with respect to calcite, colored with 0.5 ‰ methylene blue to better determine the drop borderline, was settled on a horizontal surface (for preliminary experiments cleaned glass surfaces and distilled water were used). The pictures were acquired with a very simple USB Celestron Handeld Microscope micro-camera, mounted at fixed focus height on a laboratory support, with a $20\times$ magnification and a resolution of 640×480 pixels. The focus was preliminary adjusted to measure the field of view (on a picture of a graph paper sheet or a ruler, advantageous for checking deformations as well), and thus determining the relation between pixels' size and real length on the pictures, useful for the subsequent calculation of droplet diameter (Figure 3). With this equipment we saved pictures having 6 mm of F.O.V. spread on 640-pixel width, thus attaining a 10 μm resolution.

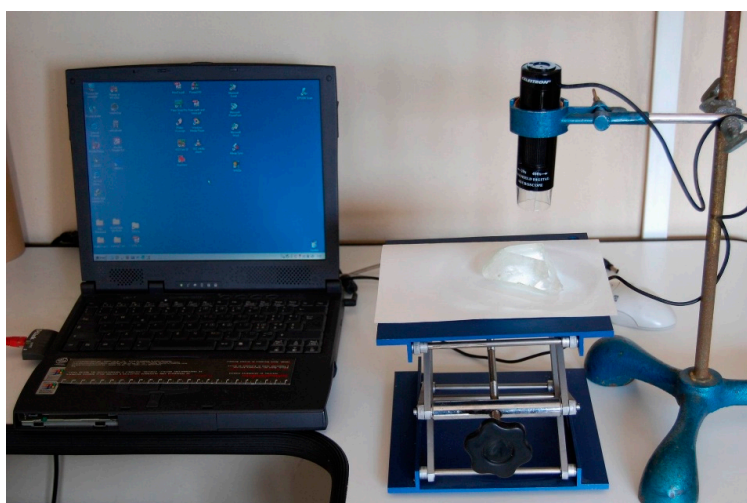


Figure 3. The simple device used to obtain a zenithal image of drops on horizontal surfaces. The handled microscope is suspended and stopped in a laboratory stand, at fixed height and fixed focus distance, previously checked. The lab screw jack is used as vertical translator stage and hosts in this picture a calcite crystal. A simple portable PC is enough to acquire the images via a USB connection.

Experiments on calcite were performed on a fresh cleavage {10.4} surface of a very pure calcite crystal. The fresh surfaces were equilibrated in air at about 296 K. The data reliability was improved by working with different droplets of the same volume, by measuring (for every drop) two different perpendicular diameters and using the averaged value for calculations. Drops of irregular shape were preliminary discarded. After each measurement, the crystal surface was washed with distilled water and dried with a gently air whisper, to avoid scratch of the surface and massive electrostatic charge generation. During two different experimental sessions, about 60 drops were photographed and measured.

2.2. Calculation of the Geometrical Parameters of the Droplets

The droplet shape should be approximately regarded as a spherical cap of diameter D , belonging to a sphere of radius R (Figure 4).

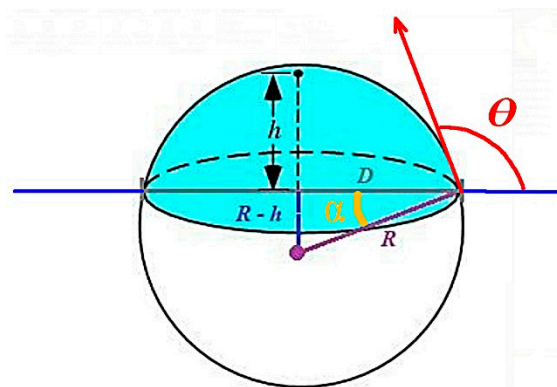


Figure 4. Droplet shape should be approximately regarded as a spherical cap of height h and diameter D , related to a sphere of radius R .

The diameter of the drop is easily obtained from a picture taken with the previously described device, having the sensor plane parallel to the solid surface (substrate, hereinafter), and the optical axis as close as possible to the symmetry axes of the droplets (in practice, with the drop in the center of the image sensor device).

To obtain θ from geometric consideration we need to obtain “ h ”, the height of the drop spherical cap on the surface. From two measurable parameters (the droplet volume V , constrained at the beginning, and the related diameter $D = 2r$), one can calculate the height (h) of the spherical cup, through the simple relation:

$$\pi h^3 + 3\pi r^2 h + 6V = 0 \quad (3)$$

This third order equations can be solved through different analytical methods, but we used a quick one, by applying free software for drawing the resulting equation, and checking the intercept value of the corresponding curve with the abscissa axis. We used an online equation grapher (Equation Grapher, [7]). From r (measured) and h (calculated) values, one gets the curvature radius R of the generating sphere:

$$R = (r^2 + h^2)/2h \quad (4)$$

Thus, one can easily obtain the angle (α):

$$\alpha = \sin^{-1}[(R - h)/R] \quad (5)$$

Finally, the contact angle θ comes out, with the precision derived from the measuring chain:

$$\theta = \alpha + \pi/2 \quad (6)$$

On the other hand, the zenithal method cannot be used for liquid/solid surface coupling with a contact angle lower than 90° , because in this case, the circumference in the contact surface is smaller than that of the superjacent droplet; hence, the circumference of the contact boundary is hidden by the drop itself. Luckily, the case of contact angle lower than 90° is rare when mineral surfaces interact with water or similar liquids.

3. Results

3.1. Stability of the Droplet

We checked the mechanical stability of the droplets during the experiment. First of all, the real shape of a liquid droplet on a solid horizontal surface is not that of a perfect spherical cap, and is affected by some deformation. This, in turn, induces some variation of the contact angle that is difficult to evaluate. Secondly, the evaporation should modify the initial volume of the droplet, and then the cap diameter D could decrease until equilibrium (saturation) is reached between the liquid and the saturated vapor phase. Performing the pictures in free air conditions, this equilibrium could not normally be reached, so the drop could undergo to complete evaporation. Experiments were performed to check the modification of the drop diameter with time. A single drop of colored distilled water was placed on a clean glass surface, and pictures of this drop were taken every minute, for a total of fifteen minutes, this time interval being considered adequate to take picture also in hostile laboratory environments. Figure 5 shows a reduced example of this sequence, from which one can argue that the strong adhesion between water and glass constrains the circumference of the drop to the fixed initial position, and the evaporation loss causes a volume reduction and convexity modification (as can be deduced by the reflected image of the lighting led on the drop surface) but nevertheless, the diameter of the spherical cap, which is the only parameter we really need to measure, is not affected at all.

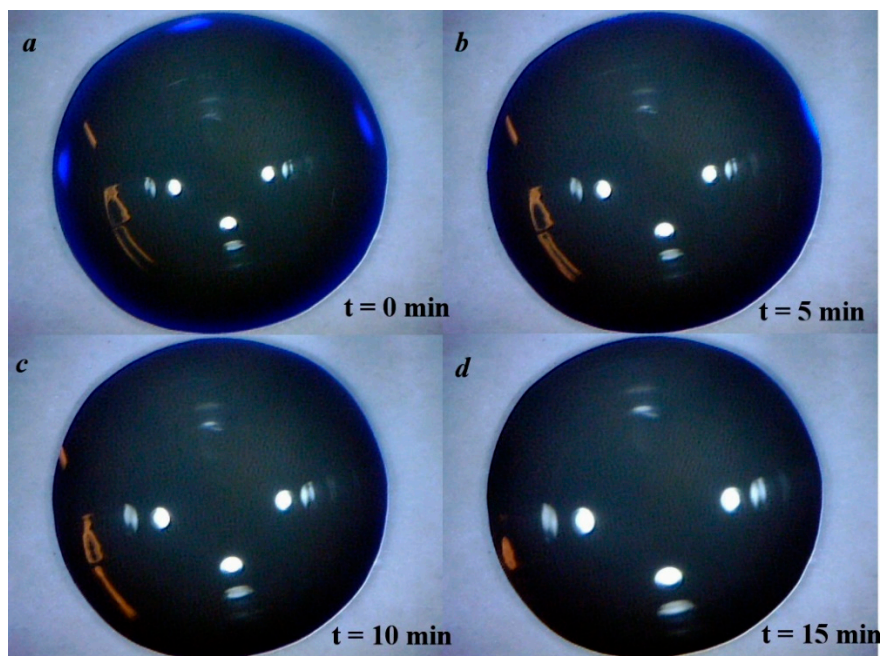


Figure 5. A spherical cap photographed at different time intervals (a–d), after its deposition on the substrate. Although evaporation occurs during time, reducing the volume and curvature of the droplet (as it could be seen by the different position of the light reflexes on the drop surface), the diameter of it remains the same for a time-lapse sufficient to capture the image. All the pictures were acquired at different times on the same droplet with the same focus and field of view (reduced by cropping to approx. 6 mm).

3.2. From the Contact Angle to the Calcite/Solution Interface Energy

We performed (in different moments) two different runs of experiments on a calcite {10.4} cleaved surface. From the first experimental series (31 drops), an averaged radius of 2.85 mm was obtained, with a dispersion comprised between 2.70 and 2.95 mm, and a relative standard deviation of 3.2%. The resulting contact angle is $\theta_1 = 146.40^\circ$. From the second run (30 drops), an average radius of 2.97 mm was obtained, with dispersion ranging between 2.80 and 3.20 mm and a relative standard deviation of 3.5%. The resulting contact angle is $\theta_2 = 131^\circ$. From this, we obtain an average contact angle of 138.70° .

From the average contact angle we obtained at the triple interface: {10.4} cleaved calcite/saturated solution/air, one can calculate the interfacial energy (γ_{sl}) at the crystal-liquid boundary using the Young's Formula (1).

At 293 K, the surface energy of water in contact with its own vapor is $\gamma_{lv} = 72.7 \text{ erg/cm}^2$. When dealing with a calcite aqueous solution saturated at room temperature, it is reasonable to adopt this γ_{lv} value, as well, owing to the very low solubility of calcite in water [8]. Calculations showed that γ_{sv} , the surface energy of {10.4}_{calcite} in vacuum at 0 K [9–13] ranges between 500 and 530 erg/cm^2 . Recently, ab initio calculations showed that at $T = 300 \text{ K}$, $\gamma_{104} = 464 \pm 18 \text{ erg/cm}^2$. Thus, here we assume this last more reliable γ_{104} value [13]. The contact angle we used is the averaged value from the two experimental sets, i.e., $\langle \theta \rangle = 138.70^\circ$.

Replacing these values in the Young's formula we obtain the surface energy calcite_{10.4}/solution: $\gamma_{sl(10.4)} = 409.38 \text{ erg/cm}^2$.

Accordingly, the adhesion energy, coming from Dupré's condition (2), corresponds to 127.32 erg/cm^2 . Then, we verified also that the limiting values (θ_1 and θ_2) of the contact angle give values of the adhesion energy compatible with the constraints of the Dupré's condition, i.e., $\beta_{adh}(\theta_1) = 120.39$ and $\beta_{adh}(\theta_2) = 133.25 \text{ erg/cm}^2$. In both cases the adhesion energy of the liquid phase is lower than the cohesion energy of the droplet, $K_{droplet} = 2\gamma_{lv} = 145.4 \text{ erg/cm}^2$.

4. Discussion

The result is largely satisfactory, since the constraints imposed by the Dupré's condition to the adhesion energy are fulfilled. To the best of our knowledge, this is the first time that an experimental value of the interface energy between the cleavage 10.4 surface and its surrounding solution fits with the theoretical prediction, obtained by ab initio calculations of the crystal/vacuum interfacial energy.

Moreover, we would like to outline once more the reliability of the measurement method we adopted. As we detailed in the Introduction, a cleavage surface, even for the best cases like that represented by the one of {10.4}_{calcite}, does not coincide with an ideal crystallographic plane, but is populated by surface defects like steps, kinks and dislocation outcrops. Quality and density of these defects vary from site to site of the surface: accordingly, the higher the number of measurements on different surface sites, the higher the approach to the real physical meaning of the measured property.

Now, to have some more data for comparison, we will compare the value we just obtained with that coming out by using the empirical formula proposed by Neumann and reported by Spelt and Li [14]:

$$\cos\theta_\gamma = -1 + 2(\gamma_{sv}/\gamma_{lv})^{1/2} \exp[-\beta(\gamma_{lv} - \gamma_{sv})^2] \quad (7)$$

where θ_γ represents the contact angle measured following the Young method, while β is a constant which was found to be $1.247 \times 10^{-4} (\text{m}^2/\text{mJ})^2$. This formula allows to determine the solid surface tension (γ_{sv}) from experimental (Young) contact angle and liquid surface tension (γ_{lv}).

When putting in Equation (4) the values of β , γ_{lv} and θ_γ , one obtains:

$$\ln(\gamma_{sv}) = 0.11735 + 2.494 \times 10^{-4}(72.7 - \gamma_{sv})^2 \quad (8)$$

which reduces to:

$$\ln(\gamma_{sv}) = 2.494 \times 10^{-4} (\gamma_{sv})^2 - 3.626 \times 10^{-2} \gamma_{sv} + 1.4355 \quad (9)$$

From the intersection of the logarithmic curve ($y = \ln\gamma_{sv}$) and the parabolic one (4c), one does find the value of $\gamma_{sv} = 218 \text{ erg/cm}^2$ which is placed almost in the middle of the range of $\{10.4\}_{\text{calcite}}$ surface energy, as reported in the literature, where we can find largely dispersed values (ranging from 70 to 1500 erg cm^{-2}) [15]. Probably, this last value, $\gamma_{sv} = 218 \text{ erg/cm}^2$, does not represent a realistic value for $\{10.4\}/\text{vacuum}$ interface; because as a matter of fact, it is not reasonable to accept that the surface energy (at 0 K) of calcite (that is made by positive (2+) and negative (2−) electrical charges) could be slightly higher than that $\gamma(100)_{\text{NaCl}} = 161 \text{ erg/cm}^2$ of a pure ionic crystal (made by positive (1+) and negative (1−) electrical charges), for faces exhibiting an analogue two-dimensional structure, as it comes out when comparing the $\{100\}$ -NaCl and the $\{10.4\}$ -CaCO₃ surfaces.

5. Conclusions

The method of zenithal imaging has some advantages and some disadvantages with respect to the classical method of lateral acquisition of the contact angle for liquid drops on a plane surface.

Advantages are the very simple experimental setup, easy-to-use apparatus, low costs, good precision in determining the geometrical parameters and quick acquisition of a large number of images to improve statistics. Disadvantages are the unusableness of the vertical acquisition when the contact angle is lower than 90°, and the necessity of a flat surface large enough to host drops of sufficient volume, a requirement that is not always easy to fulfil when dealing with natural samples.

We measured the surface energy $\gamma_{sl}^{(10.4)}$ of the calcite cleavage rhombohedron, in the presence of calcium carbonate saturated solution. The value we found through our method complies with the constraints imposed by the Dupré's formula.

In fact, from: (i) the well-known experimental value γ_{lv} of the surface energy between the solution and the vapor phase; (ii) γ_{sv} , the crystal-vapor interfacial energy, calculated at room temperature along with (iii) our experimental $\gamma_{sl(10.4)}$ value, a value has been obtained of $^{(10.4)}\beta_{\text{adh}}$, the adhesion energy between the crystal surface and the mother solution, which is compatible, for the first time, with the cohesion energy of the solution. The self-consistency of the results obtained by our method seem to be quite promising for further measurements on other crystal surfaces growing from solution.

Author Contributions: E.C. conceived and designed the experiments; E.C. performed the experiments; E.C. and D.A. analyzed the data; E.C. contributed reagents/materials/analysis tools; E.C. and D.A. wrote the paper.

Acknowledgments: The Authors wish to thank Linda Pastoro and Marco Bruno (Dip. Scienze della Terra, Università di Torino) for their kind cooperation and suggestions.

Conflicts of Interest: The authors declare no conflict of interest.

References

1. Ferrari, M.; Liggieri, L.; Miller, R. *Drops and Bubbles in Contact with Solid Surfaces*; CRC Press: Boca Raton, FL, USA, 2013; 344p., ISBN 9781466575455.
2. Hartland, S. *Surface and Interface Tension*; CRC Press: Boca Raton, FL, USA, 2004; 1500p., ISBN 9780824750343.
3. Adams, N.K. The Chemical Structure of Solid Surfaces as Deduced from Contact Angles. In *Contact Angle, Wettability, and Adhesion*; Fowkes, F.E., Ed.; ACS Publications: Washington, DC, USA, 1964; pp. 52–56, ISBN 9780841200449. [CrossRef]
4. Young, T. An Essay on the Cohesion of Fluids *Philos. Trans. R. Soc. Lond.* **1805**, *95*, 65–87. [CrossRef]
5. Schrader, M.E. Young-Dupré Revisited. *Langmuir* **2002**, *11*, 3585–3589. [CrossRef]
6. De Yoreo, J.J.; Vekilov, P.G. Principles of Crystal Nucleation and Growth. *Rev. Mineral. Geochem.* **2003**, *54*, 57–93. [CrossRef]
7. Pierce, R. 'Equation Grapher'. Math Is Fun. 2017. Available online: <http://www.mathsisfun.com/data/grapher-equation.html> (accessed on 11 February 2018).

8. Haynes, W.M. *CRC Handbook of Chemistry and Physics*, 90th ed.; CRC Press, Taylor and Francis Group: Boca Raton, FL, USA, 2010; 2610p. [[CrossRef](#)]
9. Rohl, A.L.; Wright, K.; Gale, J.D. Evidence from surface phonons for the (2×1) reconstruction of the $(10\bar{1}4)$ surface of calcite from computer simulation. *Am. Mineral.* **2003**, *88*, 921–925. [[CrossRef](#)]
10. Bruno, M.; Aquilano, D.; Pastero, L.; Prencipe, M. Structures and Surface Energies of (100) and Octopolar (111) Faces of Halite (NaCl): An Ab initio Quantum-Mechanical and Thermodynamical Study. *Cryst. Growth Des.* **2008**, *8*, 2163–2170. [[CrossRef](#)]
11. Bruno, M.; Massaro, F.R.; Prencipe, M.; Aquilano, D. Surface reconstructions and relaxation effects in a centre-symmetrical crystal: The {00.1} form of calcite (CaCO_3). *CrystEngComm* **2010**, *12*, 3626–3633. [[CrossRef](#)]
12. Akiyama, T.; Nakamura, K.; Ito, T. Atomic and electronic structures of CaCO_3 surfaces. *Phys. Rev. B* **2010**, *84*, 085428. [[CrossRef](#)]
13. Bruno, M.; Massaro, F.R.; Pastero, L.; Costa, E.; Rubbo, M.; Prencipe, M.; Aquilano, D. New Estimates of the Free Energy of Calcite/Water Interfaces for Evaluating the Equilibrium Shape and Nucleation Mechanisms. *Cryst. Growth Des.* **2013**, *13*, 1170–1179. [[CrossRef](#)]
14. Spelt, J.K.; Li, D. The equation of state approach to interfacial tension. In *Applied Surface Thermodynamics*; Marcel Dekker: New York, NY, USA, 1996; pp. 239–293, ISBN 0-8247-9096-0.
15. Forbes, T.Z.; Radha, A.V.; Navrotsky, A. The energetics of nanophase calcite. *Geochim. Cosmochim. Acta* **2011**, *75*, 7893–7905. [[CrossRef](#)]



© 2018 by the authors. Licensee MDPI, Basel, Switzerland. This article is an open access article distributed under the terms and conditions of the Creative Commons Attribution (CC BY) license (<http://creativecommons.org/licenses/by/4.0/>).